

# Monitoring nitrogen, phosphorus and sulphur in hybrid rice (*Oryza sativa* L.) using hyperspectral remote sensing

G. R. Mahajan<sup>1,4</sup> · R. N. Pandey<sup>1</sup> · R. N. Sahoo<sup>2</sup> ·  
V. K. Gupta<sup>2</sup> · S. C. Datta<sup>1</sup> · Dinesh Kumar<sup>3</sup>

Published online: 3 December 2016  
© Springer Science+Business Media New York 2016

**Abstract** Till date, the remote sensing research on crop nutrient monitoring has focused mainly on biomass and nitrogen (N) estimation and only a few attempts had been made to characterize and monitor macronutrients other than N. Field experiments were undertaken to study the remote detection of macronutrient status of rice using hyperspectral remote sensing. The variability in soil available N, phosphorus (P) and sulphur (S) and their content in plants were created using artificial fertility gradient design. The leaf and canopy hyperspectral reflectance was captured from variable macronutrient status vegetation. Linear correlation analysis between the spectral reflectance and plant nutrient status revealed significantly ( $p < 0.05$ ) higher correlation coefficient at 670, 700, 730, 1090, 1260, 1460 nm for the nutrient under study. Published and proposed vegetation indices (VIs) were tested for canopy N, P and S prediction. The results of the investigation

---

✉ G. R. Mahajan  
gopal.soil@gmail.com; gopal.mahajan@icar.gov.in

R. N. Pandey  
rnpandeyssaciari@rediffmail.com; rnpandeyssaciari@gmail.com

R. N. Sahoo  
rnsahoo.iari@gmail.com

V. K. Gupta  
vk\_001@yahoo.com

S. C. Datta  
samar1953@yahoo.com; datta.samar@gmail.com

Dinesh Kumar  
dineshctt@yahoo.com

<sup>1</sup> Division of Soil Science and Agricultural Chemistry, Indian Agricultural Research Institute, New Delhi 110012, India

<sup>2</sup> Division of Agricultural Physics, Indian Agricultural Research Institute, New Delhi 110012, India

<sup>3</sup> Division of Agronomy, Indian Agricultural Research Institute, New Delhi 110012, India

<sup>4</sup> Present Address: Section of Natural Resource Management, ICAR - Indian Council for Agricultural Research Complex for Goa, Old Goa, Goa 110012, India

revealed that, published VIs (NDVI hyper and NDVI broadbands) could retrieve canopy N with higher accuracy, but not P and S. The predictability of the visible and short wave infrared based VI  $NRI_{1510} ((R_{1510} - R_{660})/(R_{1510} + R_{660}))$  was the highest ( $r = 0.81$ ,  $p < 0.01$ ) for predicting N. Based on the outcomes of linear correlation analysis new VIs were proposed for remote detection of P and S. Proposed VI  $P_{670\_1260} ((R_{1260} - R_{670})/(R_{1260} + R_{670}))$  retrieved canopy P status with higher prediction accuracy ( $r = 0.67$ ,  $p < 0.01$ ), whereas significantly higher canopy S prediction ( $r = 0.58$ ,  $p < 0.01$ ) was obtained using VI  $S_{670\_1090} ((R_{1090} - R_{670})/(R_{1090} + R_{670}))$ . The proposed spectral algorithms could be used for real time and site-specific N, P and S management in rice. Nutrient specific wavelengths, identified in the present investigation, could be used for developing relatively low-cost sensors of hand-held instruments to monitor N, P and S status of rice plant.

**Keywords** Hyperspectral remote sensing · Nitrogen · *Oryza sativa* L. · Phosphorus · Spectroradiometer · Sulphur

## Introduction

Rice is one of the most important staple foods for two third population of the world. In India, rice crop productivity is lower ( $3.65 \text{ t ha}^{-1}$ ) when compared to the world's average productivity ( $4.52 \text{ t ha}^{-1}$ ) (FAOSTAT, 2015). The causes of lower yield of rice in context of the present investigation are imbalanced use of fertilizers and the emerging nutrient deficiencies. The Indian agriculture is operating at net negative nutrient balance with the estimated net negative nitrogen (N), phosphorus (P) and potassium (K) (NPK) balance from net sown area being  $69 \text{ kg ha}^{-1}$  ( $16 \text{ kg N ha}^{-1} \text{ year}^{-1} + 11 \text{ kg P ha}^{-1} \text{ year}^{-1} + 42 \text{ kg K ha}^{-1} \text{ year}^{-1}$ ) (Tandon 2004). There are 23, 14 and 5 countries in Africa with net NPK balance with worse than  $-60 \text{ kg ha}^{-1} \text{ year}^{-1}$ , between  $-30$  and  $-60 \text{ kg ha}^{-1} \text{ year}^{-1}$  and better than  $-30 \text{ kg ha}^{-1} \text{ year}^{-1}$ , respectively (Henao and Baanate 1999). Whereas the negative N, P and K balance globally was estimated as 18.7, 5.1 and  $38.8 \text{ kg ha}^{-1} \text{ year}^{-1}$ , respectively (Tan et al. 2005). Studies on nutrient balance in different countries, viz. sub-Saharan Africa, Africa, China, Ghana, Kenya, Mali was shown to have a negative balance for N ( $-12$  to  $-8 \text{ kg ha}^{-1} \text{ year}^{-1}$ ), P ( $-4.5$  to  $0 \text{ kg ha}^{-1} \text{ year}^{-1}$ ) and K ( $-62$  to  $-15 \text{ kg ha}^{-1} \text{ year}^{-1}$ ) (FAO 2003; Sheldrick et al. 2003; Stoorvogel and Smaling 1990). While the reasons for negative nutrient balance are use of imbalanced fertilizers and unavailability of an adequate amount of fertilizers, there remains a focus on more production of fertilizers. Furthermore, producing more quantity with same or less amount of fertilizers would be a sustainable strategy to tackle this problem. The major outcome of the negative nutrient balance is emerging nutrient deficiencies in different crop plants and reduced yield. Under such circumstances, one of the pragmatic options is to improve the nutrient use efficiency and this compels adoption efficient techniques and machineries. Traditional methods for detecting and monitoring essential nutrients in plants needs detailed sampling, time and expensive laboratory chemical analyses; this is neither economically viable nor environmentally acceptable on a large scale (for instance individual farmer's field). Moreover, several physical processes already disrupt by nutrient stress, by the time the plant nutrient deficiency symptoms become clearly visible (Zhao et al. 2003). The net negative nutrient balances could be addressed by producing more with

lesser input. The crop plant nutrient demand and supply could be achieved by adopting remote sensing based real time methods with large area nutrient detection in plants. Consequently timely detection or forewarning of nutrient stress could help avoid deficiencies and yield loss in plants.

Difference in colouration and production of different chemical compounds due to deficiency or sufficiency of N, P, K and S in plants alters spectral reflectance pattern of the leaves or canopy. The different absorption bands corresponding to the structure or molecules reviewed from literature could be paired as: 460 and 670 nm—chlorophyll *a* and *b*, 530 nm—carotenoids, (Osborne et al. 1993; Zur et al. 2000) and 1500 nm—N–H bond (Curran 1989). This makes nutritional monitoring of crop plants using remote sensing possible. A characteristic absorption feature of disulfide bond is present in the visible (VIS) region (500–600 nm). Thus monitoring the variability of N, P and S in plants using the above-mentioned features is an important component of precision agriculture. Precision agriculture is one of the top ten revolutions in agriculture (Crookston 2006; Mulla 2013). Precision agriculture involves better management of farm inputs, say fertilizer nutrients (Crookston 2006; Mulla 2013). On the contrary, conventional management deals with uniform application of fertilizer nutrients. Using precision agriculture a field can be divided into management zones receiving customized management inputs based on varying soil types, landscape position and management history (Mulla 2013). In context of precision farming, quantitative information on plant nutrient concentration is very important to plan strategic application of fertilizers (Stroppiana et al. 2009). But, this requires cost and time-effective methods to identify and evaluate crop conditions to recommend suitable measures (Ryu et al. 2009). Moreover, precision agriculture needs to provide information on spatial variation and since temporal variation might not be achieved on real time (Steven 2004). To confront the current pressure of optimizing agricultural production and lower input use efficiency, agricultural industry is adopting information technology as a new tool (Pimstein et al. 2011). Crop stress monitoring is one of the important utilities of remote sensing (Prabhakar et al. 2011). It has a great potential because it enables wide area, non-destructive and real time acquisition of information on crop plant condition (Inoue 2003). There are a number of methods proposed for in situ and non-destructive estimation of plant nutritional status like leaf colour chart and chlorophyll meters, but these methods focus on the individual leaves and thus pose difficulty in reflecting a population nutritional status (Feng et al. 2008). In contrast, the hyperspectral reflectance collected from canopy has the capacity to detect representative population nutrition status rather than individual leaf or plant (Feng et al. 2008). Processing of hyperspectral remote sensing data can be categorized into three groups (1) Narrow band or hyperspectral vegetation indices (VIs) (2) multivariate data analysis (Inoue and Penuelas 2001) and (3) hyperspectral data as a base for wide band VIs. Different statistical approaches employed for radiometric data processing to characterize the plant macronutrient status have been given in Table 1 chronologically. From Table 1, it is evident that the monitoring of macronutrient status in different crops using remote sensing approaches is possible, however, very little information for rice crop (except N) is available. Owing to the importance of N, P and S in bringing better rice yield and quality, very little attention has been given to their remote detection using remote sensing. This emphasizes a need to develop robust and more specific algorithms for prediction of P and S status in rice crop.

The present investigation was aimed (1) to analyze the relationships of leaf and canopy N–P–S concentrations with their respective hyperspectral reflectance to identify N–P–S responsive wavelength(s) and (2) to identify the VIs with the better predictive capacity for N–P–S in rice.

**Table 1** Advances in macro- and micro-nutrient monitoring using remote sensing

Crop	Nutrients	Data analysis technique	Result or inference	Reference
Grasses	N	Non-linear PLSR	$R^2 = 0.81$ and $RMSE = 0.08$	Ramoelo et al. (2013)
	P	Non-linear PLSR	$R^2 = 0.80$ and $RMSE = 0.03$	
Rape (oilseed)	N	LS-SVM	$r = 0.88$	Zhang et al. (2013)
	P	LS-SVM	$r = 0.71$	
Savanna grassland	N, P and Fibre	Principle component analysis involving ancillary and absorption variable	$R^2_{adj} = 0.49-0.74$ and lowest RMSE	Knox et al. (2012)
Litchi		Regression equations of first order derivative of reciprocal-logarithmic-transformed reflectance ( $\log(1/R)$ ) at following wavelengths		Chen et al. (2011)
Wheat	Ca	1018 nm	$R^2 = 0.74$ and $RMSE = 0.748\%$	
	Mg	1601 nm	$R^2 = 0.64$ and $RMSE = 0.001\%$	
	P (concentration)	Vegetation index N_1645_1715	$r = 0.55$ and $RMSE = 0.017\%$	Pimstein et al. (2011)
	P (concentration)	PLSR (Selective wavelengths)	$r \geq 0.42$ and $RMSE = 0.017-0.062\%$	
	P (content)		$r \geq 0.71$ and $RMSE = 0.178-0.387 \text{ g m}^{-2}$	
Potato	N	SWIR based vegetation index, $NR_{1510} = (R_{1510} - R_{660}) / (R_{1510} + R_{660})$	$R^2 = 0.59$ ( $p < 0.005$ ) and $RMSE = 0.421\%$	Herrmann et al. (2010)
Deciduous orchard (Pear, Cherry, peach, apricot)	N	Step-wise regression analysis method,	$R^2 = 0.47-0.99$	Basyigit and Senol (2009)
	P	multiple linear regression equations of selected wavelengths	$R^2 = 0.73-0.99$	
	Mg		$R^2 = 0.58-0.99$	
	Mn		$R^2 = 0.60-0.99$	
	Ca		$R^2 = 0.10-0.99$	
	Fe		$R^2 = 0.37-0.98$	
	Zn		$R^2 = 0.25-0.99$	
Cu		$R^2 = 0.22-0.99$		

Table 1 continued

Crop	Nutrients	Data analysis technique	Result or inference	Reference
Cucumber leaf	P	Selection of P sensitive wavelengths using stepwise multi-regression—978, 920, 737 and 458 nm; Artificial neural network (ANN) Support vector machine (SVM)	Calibration accuracy: 0.995 Validation accuracy: 0.712 Calibration accuracy: close to 1.00 Validation accuracy: 0.754	Zhang and Li (2008)
Olive	N	Discriminant analysis Wavelengths in NIR region (from 710–900 nm) were used to discriminate N stress	Accuracy of up to 99.2%	Gomez-Casero et al. (2007)
Barley	N, P and K	Stepwise multi-way PLSR model analysis with dummy variables	Discrimination with 92% accuracy	Jorgensen et al. (2007)
Wheat	N, P, K, Ca and Mg	Percentage decrease in reflectance in VIS and NIR domain of energy spectrum	Spectral properties are useful in early mineral nutrient deficiency detection but to know specific nutrient deficiency is difficult	Ayala-silva and Beyl (2005)
Corn (before V8 stage)	N and Mg P	Red-edge shift to shorter wavelengths Linear models of wavelength in blue (440 and 445 nm) and NIR (730 and 930 nm) range	$R^2 = 0.37-0.88$	Osborne et al. (2002)

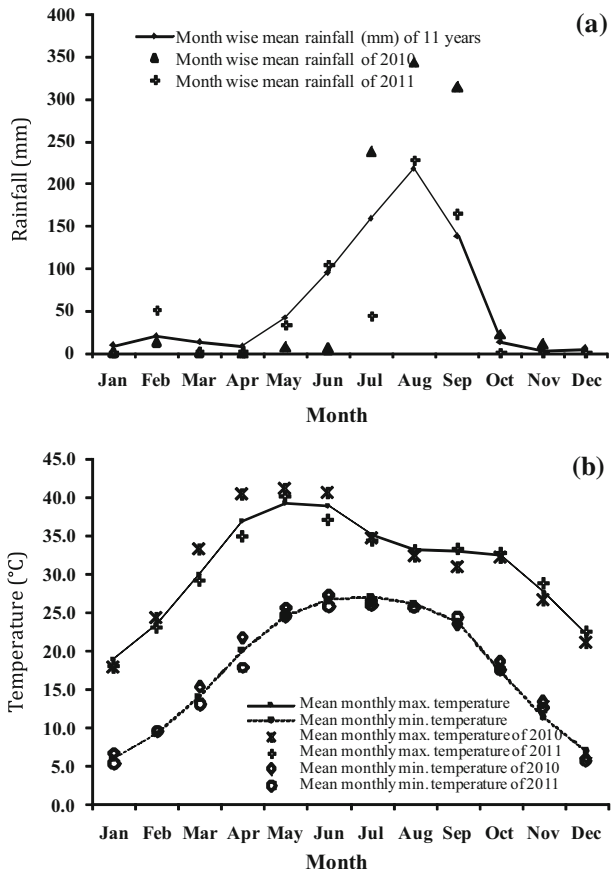
PLSR partial least square regression,  $R^2$  regression coefficient,  $RMSE$  root means square error,  $LS$ -SVM least square support vector machine,  $r$  correlation coefficient,  $R^2_{adj}$  adjusted  $R^2$

## Materials and methods

### Details of the experimental site

A test field at the research farm of the Indian Agricultural Research Institute, New Delhi, India (28.4°N, 77.1°E and 250 m above the mean sea level) was selected. The soil of the experimental field was taxonomically categorized under *Typic Haplusteps* (Old alluvium), predominant in illitic type clay mineral and sandy loam in texture. The soil of the experimental field was characterized for electro-chemical and soil available nutrients before start of the experiment. The soil of the experimental field had 166 kg ha<sup>-1</sup> alkaline permanganate oxidizable N (Subbiah and Asija 1956), 14 kg ha<sup>-1</sup> 0.5 N sodium bicarbonate-extractable P (Olsen et al. 1954), 146 kg ha<sup>-1</sup> neutral N ammonium acetate exchangeable K (Hanway and Heidel 1952), 22 kg ha<sup>-1</sup> 0.15% CaCl<sub>2</sub> extractable-S (Williams and Steinbergs 1959), 0.43% organic carbon (Walkley and Black 1934), pH 8.0 and electrical conductivity 0.43 dS m<sup>-1</sup> in 1:2.5 soil to water suspension ratio (Jackson 1973) before start of the experiments. Diphenyl triamine pentaacetic acid (DTPA)—extractable micronutrients (Lindsay and Norvell 1978)—Fe, Mn, Zn and Cu were present in sufficiency range of availability. So, no additional micronutrient application was made.

**Fig. 1** Month wise mean **a** rainfall and **b** maximum and minimum temperature of 11 years from 2002 to 2012 and years of experimentation i.e. 2010 and 2011 at IARI experimental farm, New Delhi, India



The month wise mean (from 2002 to 2012) of the maximum and minimum temperature and rainfall are presented as Fig. 1.

### Induction of fertility gradient prior to test crop experiment

Creating nutrient variability in the experimental plots and the plants is a major pre-requisite for studying the hyperspectral reflectance pattern from vegetation. In order to achieve this artificial fertility gradient was created before the test crop experiments following inductive methodology by Ramamoorthy et al. (1967). The design developed by All India Coordinated Research Project on Soil Test Crop Response, Indian Council of Agricultural Research was adopted to conduct the study. The field was divided into three equal rectangular strips and fertilizer N, P and S were applied as  $N_0P_0S_0$  (strip I),  $N_{1/2}P_{1/2}S_{1/2}$  (strip II) and  $N_1P_1S_1$  (strip III) where  $N_1P_1S_1$  represents 400, 300 and 150 kg ha<sup>-1</sup> of N, P<sub>2</sub>O<sub>5</sub> and S, respectively (Fig. 2). The soil fertility gradient with respect to farmyard

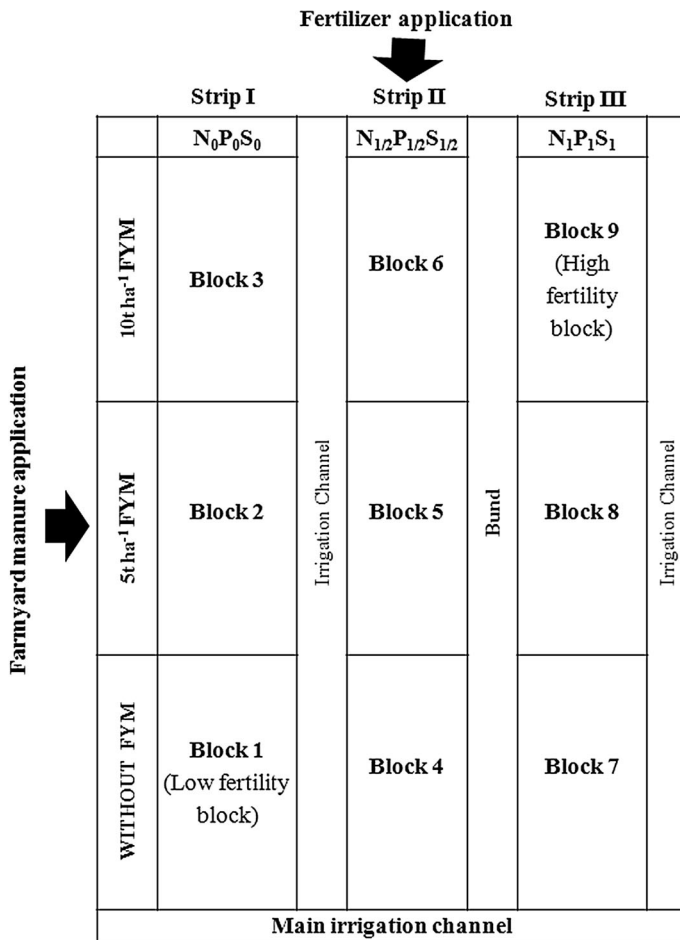


**Fig. 2** Layout for creating fertility gradient in the experimental field. Where,  $N_0P_0S_0$ ,  $N_{1/2}P_{1/2}S_{1/2}$  and  $N_1P_1S_1$  represent no, medium and high dose of fertilizer NPS applied to strip I, strip II and strip III, respectively,  $N_1P_1S_1$  represents 400, 300, 150 kg ha<sup>-1</sup> of N, P<sub>2</sub>O<sub>5</sub> and S, respectively

manure (FYM) was developed by applying FYM @ 0, 5 and 10 t ha<sup>-1</sup> in three strips across the fertilizer strips. A preliminary exhaustive fodder maize crop (variety: African tall) was grown to stabilize soil fertility during summer 2010 and it was then harvested as a fodder. The major aim of inducing the fertility gradient was to create significant variability with respect to the soil available N, P and S prior to test crop experimentation. The results of the fertility gradient experiment are furnished in Fig. 4 as descriptive statistics of soil available N, P and S. In general, the mean values of alkaline KMnO<sub>4</sub>-N, Olsen's-P and 0.15% CaCl<sub>2</sub> extractable-S were observed as strip III > strip II > strip I. A higher gradient of 43, 81 and 92% for KMnO<sub>4</sub>-N, Olsen's-P and 0.15% CaCl<sub>2</sub> extractable-S was observed in strip III over strip I. Fertility gradient built up among strip was expected because strip III was highly fertilized strip compared to strip I which received no fertilizer nutrients. The range of the alkaline KMnO<sub>4</sub>-N, Olsen's-P and 0.15% CaCl<sub>2</sub> extractable-S during both the years of the experimentation was 132–232 kg ha<sup>-1</sup> (Deficient), 11.0–32.3 kg ha<sup>-1</sup> (Deficient to Sufficient) and 16.4–40.9 kg ha<sup>-1</sup> (Deficient to Sufficient), respectively (Fig. 3). Within strip fertility gradient built up was also noticed by across strip FYM application. Within strip variations in fertility is conspicuous from the values of coefficient of variation (CV), the order was as P > S > N during both the years of experimentation (Fig. 3). The results of the fertility gradient methodology indicated the development of an adequate variability with respect to soil available N, P and S before start of test crop experimentation.

### Test crop experimentation

After ensuring the development of fertility gradient, nine distinctly different fertility blocks (three within each strip) were obtained. Total of 24 treatments (eight within each block containing one untreated control) were assigned, randomized and replicated thrice making the total of 72 plots. The size of individual plot was 14.26 m<sup>2</sup> (6.2 × 2.3 m<sup>2</sup>). The experiment was laid out in 'fractional factorial randomized block design' (Fig. 4). The treatments consisted of various selected combinations of four levels of nitrogen (0, 70, 140 and 210 kg N ha<sup>-1</sup>), phosphorus (0, 30, 60 and 90 kg P<sub>2</sub>O<sub>5</sub> ha<sup>-1</sup>) and sulphur (0, 15, 30 and 45 kg S ha<sup>-1</sup>) and three levels of FYM (0, 5 and 10 t FYM ha<sup>-1</sup>). Treatments were randomized in each of the three strips in such a way that all the 24 (21 treated + 3 untreated control) treatments were present in all three strips in either direction (Fig. 3). Fertilizer N was applied in three equal splits one basally and two top dressings at tillering and panicle initiation and P and S was applied before transplanting. Test crop aromatic

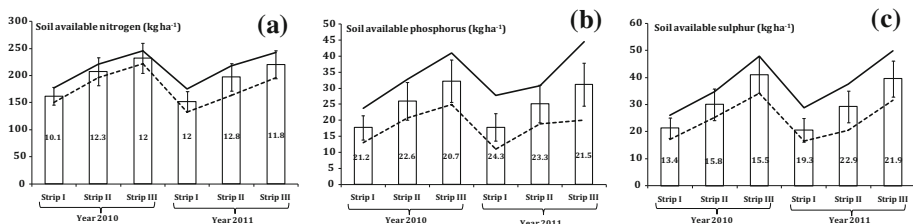


**Fig. 3** Variability of soil available **a** nitrogen (N), **b** phosphorus (P) and **c** sulphur (S) (kg ha<sup>-1</sup>) in three different strips before start of the experiments in year 2010 and 2011. The *black continuous* and *dotted line* represents the maximum and minimum values of the respective parameters, respectively. The *error bars* represents the standard deviation (kg ha<sup>-1</sup>) whereas the *values inside the bars* are coefficient of variation (expressed as %)



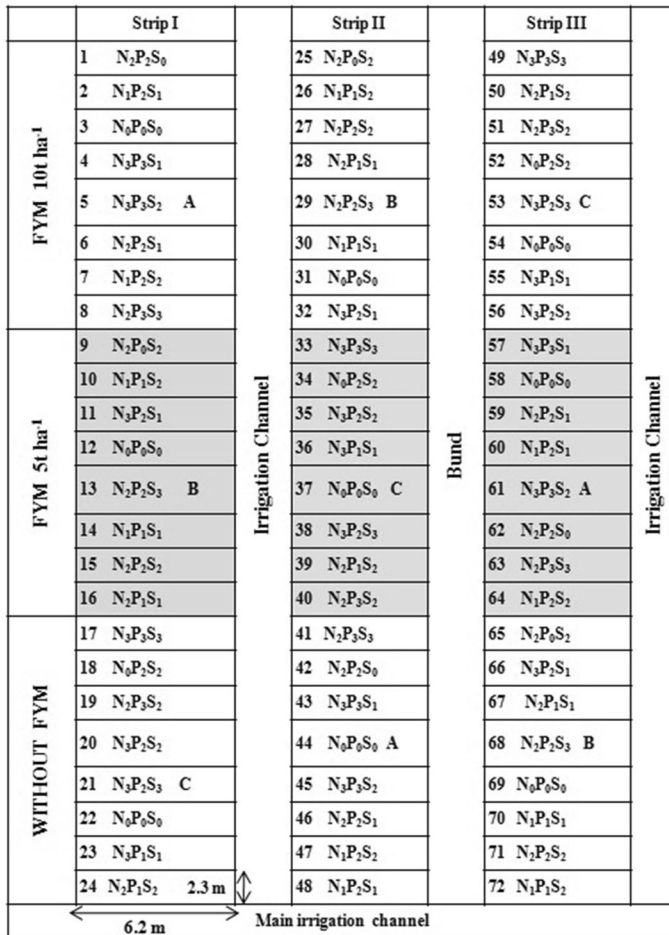


**Fig. 4** Layout for the test crop experiment. Where (1) N<sub>0</sub>, N<sub>1</sub>, N<sub>2</sub> and N<sub>3</sub> means 0, 60, 120 and 180 kg N ha<sup>-1</sup>, respectively, (2) P<sub>0</sub>, P<sub>1</sub>, P<sub>2</sub> and P<sub>3</sub> means 0, 30, 60, 90 kg P<sub>2</sub>O<sub>5</sub> ha<sup>-1</sup>, respectively and (3) S<sub>0</sub>, S<sub>1</sub>, S<sub>2</sub> and S<sub>3</sub> means 0, 15, 30, 45 kg S ha<sup>-1</sup>, respectively. Three different blocks of eight treatments A, B and C were randomized in three different strip

hybrid rice ‘Pusa Rice Hybrid-10’ (PRH-10) was grown as a component of hybrid rice–wheat cropping system during wet seasons of 2010 and 2011 on the same site of the previous fertility gradient experiment. ‘PRH-10’ is world’s first aromatic rice hybrid developed by Indian Agricultural Research Institute, New Delhi, India. The experimental field was ploughed by tractor-drawn disc harrow which was then levelled once using laser leveller before start of the experiment in 2010. The levelled field was puddled twice using tractor-drawn puddler in standing water in both the years. Seedlings were transplanted in first week of July 2010 and second week of July 2011 at a spacing of 20 cm × 15 cm in 6.2 m × 2.3 m size plots. Basal dose of N were applied in four equal splits at basal, tillering, panicle initiation and flowering stages of rice. Basal doses of P and S were applied before transplanting in all the plots in both the years. Twenty two days old two seedlings per hill were transplanted in standing water after puddling. Standing water of 5 cm was

maintained throughout the growing season in all the plots. Dikes were sufficiently high and compacted enough to prevent seepage, overflow of water and transfer of nutrients into and from adjacent plots. Weed management and plant protection measures were followed uniformly in all the plots as and when required. Crop was harvested in second week of October in 2010 and third week of October in 2011.

### Radiometric observations

The hyperspectral reflectance of the rice crop canopy at the panicle initiation stage was recorded with handheld Analytical Spectral Devices (ASD) Fieldspec 3 spectroradiometer over 350–2500 nm wavelength range with 25° field of view. Spectral resolution of the spectroradiometer was 3 nm in the VIS and 8 nm in the NIR range of the spectrum. The resultant data was processed using ViewSpecPro software to produce values at each nanometer interval. Canopy reflectance was recorded between 11:00 a.m. to 1:00 p.m. local time under cloudless condition. The spectroradiometer was allowed to warm up for 30 min before recording the actual observations. Optimization of the instrument was done periodically using a standard white reference panel (Spectralon Labsphere Inc., North Sutton, NH, USA). After every capturing spectral signature of 12 plots, referencing using the white reference panel was done, which was as well done before starting the next capture in case of occurrence of the unclear sky or cloudy situation. The spectroradiometer was set to average the five captures, thus five spectral signatures per unit treatment were captured. Leaving two border rows out of observation, five spectral signatures—four at the corner and one at centre were obtained in each of the treatment. The spectral reflectance was recorded at a uniform height of 1 m above the canopy to maintain uniform canopy coverage under the each observation throughout the plots. The flag leaf samples were picked and transported in the paper bags. The flag leaf is the youngest leaf of rice plant from which the panicle emerges. A total of 25 flag leaves were collected per treatment and grouped in five samples. Before capturing the spectral signature, the samples were washed with distilled water and dried using blotting paper to avoid spectral interference due to moisture. An average of five leaf spectral signatures from one composite sample per plot was considered as a representative spectral signature. The leaf spectral signature was obtained from the middle of the picked flag leaves. Since the rice leaves were too narrow to cover the opening of contact probe of the spectroradiometer, more than one representative leaf samples were chosen and spread on a white surface and reflectance was recorded so that only reflectance from leaf will be recorded. The flag leaf reflectance was recorded using a contact probe of the same instrument in a Hyperspectral Laboratory (dark room). This exercise was done in the dark condition to avoid any spectral interference due to stray light while capturing the spectral signature. The aim of capturing the flag leaf reflectance was to get pure spectral signature to identify the nutrient sensitive wavelengths in some selected section of the energy spectrum, which would otherwise not be possible using canopy spectral signatures. A total of 144 leaf and 144 canopy spectral signatures (72 during each year of experimentation) were captured. One representative spectral signature (average of five) for canopy and leaf per treatment was considered for the statistical analysis. Atmospheric water absorption spectral regions (1350–1450 and 1750–1980 nm) and the spectral reflectance data from 350 to 400 nm were omitted to avoid distortion of the signals (Yi et al. 2007).

## Plant sampling and chemical analysis

The leaf and whole plant samples were collected separately from each plot spectral data collection (0.5 m × 0.5 m) at the panicle initiation stage for determination of dry biomass and nutrient concentration on dry weight basis. The plant samples were collected immediately after recording the spectral reflectance data. The samples were then oven dried ( $60 \pm 2$  °C) till the constant weight was attained and ground for further chemical analysis. The samples were digested in di-acid mixture ( $\text{HNO}_3:\text{HClO}_4 = 9:4$  v/v) for the chemical analysis of phosphorus and sulphur (Jackson 1973). The total P concentration in the digest was determined spectrophotometrically using vanado-molybdate phosphoric acid yellow colour method (Jackson 1973). Total S in the digest was determined spectrophotometrically by developing turbidity using  $\text{BaCl}_2$  (Tabatabai and Bremer 1970). Total N concentration in the leaf and plant samples were analysed by modified micro Kjeldahls' method (Yoshida et al. 1976). The macronutrient variability in the leaf and canopy was characterized by standard deviation and coefficient of variation (CV, expressed as a percentage) ( $\text{Standard deviation}/\text{Mean} \times 100$ ) (%).

## Data analysis

### *Analysis of spectral data*

The raw digital numbers (DN) values recorded using the spectroradiometer were converted to the spectral reflectance values using the ASD ViewSpecPro software. The data was analyzed for effect of variable N, P and S status of plants on the spectral reflectance response at leaf and canopy level. The objective was to identify regions of the spectrum where the reflectance is most sensitive to variable N, P and S status of the leaves and canopy. In order to identify the significant and nutrient-sensitive wavelengths, correlation coefficients at 5% of the level of confidence for leaf as well as canopy reflectance were computed. Specific wavelengths showing significant positive or negative correlation were selected for developing newer spectral algorithms.

### *Vegetation indices*

Published hyperspectral and narrow band VIs reviewed in literature (Table 2) and proposed in the present study were evaluated for their ability to characterize N, P and S status in rice. Correlation analysis was performed between the leaf and canopy spectral reflectance and plant macronutrient concentration. This was done to identify and select wavelength(s) and wavebands responsive to variable macronutrient concentration in rice plant. The pooled dataset from both the years of experimentation ( $n = 144$ ) had been used for this purpose. The new spectral algorithms, i.e. VIs were proposed as a normalized configuration of selected wavelengths based on the outcomes of the linear correlation analysis. The data was divided year wise for development of models. Regressive calibration models (single and combined-year) of the VIs and nutrient concentration were calibrated using the calibration dataset (2010, 2011 and 2010/11 dataset). No same samples were used for the calibration and cross validation in case of the single year model. The cross validation combinations as—2010 calibration model validated on 2011 dataset, 2011 calibration model validated on 2010 dataset, combined (2010–2011) calibration model validated on 2010 dataset and combined (2010–2011) calibration model validated on 2011 dataset were

**Table 2** Traditional vegetation indices studied in present study

Vegetation index	Formula	Reference
Normalized Difference Vegetation Index (NDVI) large	$(R_{800-900} - R_{650-700}) / (R_{800-900} + R_{650-700})$	Rouse et al. (1974)
Normalized Difference Vegetation Index (NDVI) hyper	$(R_{800} - R_{680}) / (R_{800} + R_{680})$	Blackburn (1998)
Green Normalized Difference Vegetation Index (GNDVI)	$(R_{800-900} - R_{540-560}) / (R_{800-900} + R_{540-560})$	Gitelson et al. (1996)
Soil Adjusted Vegetation Index (SAVI)	$((R_{800-900} - R_{650-700}) / (R_{800-900} + R_{650-700} + 0.5)) (1 + 0.5)$	Huete (1988)
Optimized Soil Adjusted Vegetation Index (OSAVI)	$(1 + 0.16) (R_{800} - R_{670}) / (R_{800} + R_{670} + 0.16)$	Rondeaux et al. (1996)
N <sub>1645_1715</sub>	$(R_{1645} - R_{1715}) / (R_{1645} + R_{1715})$	Pimstein et al. (2011)
NRI <sub>1510</sub>	$(R_{1510} - R_{660}) / (R_{1510} + R_{660})$	Herrmann et al. (2010)

*R* reflectance at corresponding subscripted wavelength (nm)

done and designated as 2010-to-2011 cross validation, 2011-to-2010 cross validation, combined-to-2010 validation and combined-to-2011 validation, respectively. The ability of the published and developed VIs to predict nutrient concentration in leaf and canopy was evaluated. The correlation coefficient (*r*), root mean square error (RMSE), relative error (RE) and ratio of performance to the deviation (RPD) were calculated to compare their prediction accuracy (Herrmann et al. 2010; Pimstein et al. 2011; Ranjan et al. 2012).

The goodness of fit of regressive models was tested based on the RMSE (Eq. 1) of prediction and RE (Eq. 2) values.

$$RMSE = \sqrt{\frac{\sum_{i=1}^n (A_i - P_i)^2}{n}} \tag{1}$$

$$RE = \sqrt{\frac{\sum_{i=1}^n ((A_i - P_i) / A_i)^2}{n}} \times 100 \tag{2}$$

where, *A<sub>i</sub>* and *P<sub>i</sub>* are the actual and predicted nutrient concentration of *i*th data point and *n* is the number of data points. The RMSE indicates closeness between actual and predicted values, with lower the RMSE, better the predictability of the model. Relative difference between actual and predicted values was indicated by RE (Eq. 2), expressed in percentage terms. Predictions were considered excellent if RE is <10%, good between 10–20%, fair between 20–30% and poor if it is > 30% (Jamieson et al. 1991).

A ratio of performance to deviation (RPD) (Eq. 3) indicates appropriateness of prediction. RPD is ratio of standard deviation of validation sample data and standard error of prediction (SEP) (Eq. 4) (Williams and Norris, 1987)

$$RPD = \frac{SD}{SEP} \tag{3}$$

where,

$$SEP = \sqrt{\frac{\sum_{i=1}^n (A_i - P_i)^2}{n - 1}} \quad (4)$$

The RPD value less than 1 indicates irrelevant prediction; between 2 and 3 indicates an adequate screening method; and greater than 3 indicate satisfactory prediction for analytical method (Malley et al. 2000).

## Statistical analysis

The statistical analysis of the data was done using the Microsoft Excel (Microsoft Corporation, USA) and SAS (Version 9.3) (SAS Institute, 2012).

## Results and discussion

### Macronutrient concentration variability

At the flag leaf level, P and S concentration were similar during 2010 and 2011. But, nitrogen concentration in 2011 was 1.19 times that in 2010 (Fig. 5). Improvement in N uptake during second year experimentation could be due to residual soil N of first year and owing to the applied N in second year. The CV for macronutrients in flag leaf was  $\geq 11.7\%$ . In comparison to flag leaf, higher variability ( $CV \geq 15.9\%$ ) was observed in canopy macronutrient concentration. Range of N and P concentrations in canopy were similar during both the years of experimentation. Whereas, S concentration during 2011 was 1.44 times higher than that in 2010.

### Cross-correlation between macronutrient concentrations

For selection of a specific dataset for linear correlation analysis between the hyperspectral reflectance and macronutrient status, presence of an adequate variability is just not sufficient. It is important to study cross-correlation between these parameters. A specific dataset showing lower or weaker cross-correlation between macronutrient concentrations should be selected for this purpose (Pimstein et al. 2011). All the parameters correlated positively and significantly with each other in cross-correlation results at panicle initiation stage (Table 3). The correlation between the flag leaf N–P–S concentration was higher than the

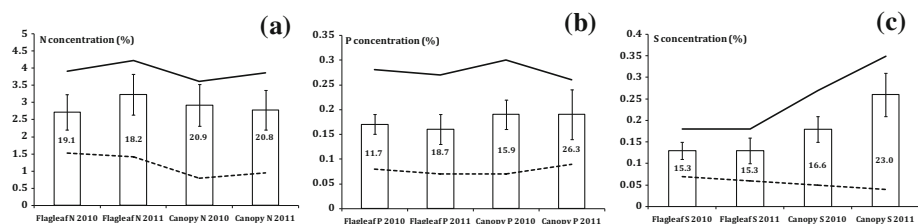


**Fig. 5** Variability of **a** nitrogen (N), **b** phosphorus (P) and **c** sulphur (S) concentration (%) in the rice flag leaf and canopy year 2010 and 2011. The black continuous and dotted line represents the maximum and minimum values of the respective parameters, respectively. The error bars represents the standard deviation (%) whereas the values inside the bars are coefficient of variation (expressed as %)

**Table 3** Cross-correlation between N, P and S concentration in flag leaf and canopy at panicle initiation stage of rice during 2010 and 2011

All the correlation coefficients are significant at 0.05 level of significance

	Flag leaf			Canopy		
	N (%)	P (%)	S (%)	N (%)	P (%)	S (%)
2010						
N (%)	1.00			1.00		
P (%)	0.69	1.00		0.51	1.00	
S (%)	0.67	0.54	1.00	0.62	0.52	1.00
2011						
N (%)	1.00			1.00		
P (%)	0.68	1.00		0.48	1.00	
S (%)	0.66	0.50	1.00	0.59	0.53	1.00

canopy N–P–S correlation. The highest correlation was observed between the flag leaf N and P ( $r = 0.68$ – $0.69$ ). The canopy N, P and S concentration showed weaker correlation with each other during 2010 ( $r \leq 0.62$ ) and 2011 ( $r \leq 0.59$ ) (Table 5). Pimstein et al. (2011) chose the dataset having N–P–K cross correlation of 0.52–0.65. Mahajan et al. (2014) considered N–P–S–K dataset with cross-correlation of 0.25–0.57 for linear correlation analyses studies. This suggests suitability of the datasets from both the years of experimentation for identification of nutrient sensitive wavelengths. To achieve this, datasets of 2010 and 2011 were pooled together and linear correlation analysis between nutrient concentration and the hyperspectral reflectance was performed.

### Macronutrient concentration and leaf reflectance

In the VIS as well as near infrared (NIR) ranges, values of correlation coefficient were negative, whereas those were positive in the shortwave infrared (SWIR) region (Fig. 5). Higher negative and significant correlation coefficients were observed for the flag leaf N and S in the VIS and NIR region, respectively. Like VIS, the NIR region showed significant correlation with N–P–S concentration. At the flag leaf level, none of the nutrient in question showed significant correlation with flag leaf reflectance in the SWIR region, except P in a specific section between 1900–2100 nm. Stronger correlation between P concentration of wheat and the spectral reflectance at 1400–1500 and 1900–2100 nm (Pimstein et al. 2011) and 1650–1710 nm (Mahajan et al. 2014) have been reported recently. This region of the spectrum could be the potential region for developing spectral algorithms for P monitoring in rice. One of the interesting facts from linear correlation analysis is that, N and P correlations followed similar pattern over the entire spectral range suggesting presence of cross-correlation between these two nutrients. The highest S correlation ( $r = 0.46$ ,  $p < 0.05$ ) was observed at slightly higher wavelength (730 nm) than N and P (700 nm). This result might be helpful to allow better understanding the relations among S and N and P by their influence on vegetation spectra in the red edge region.

### Macronutrient concentration and canopy reflectance

We observe from Fig. 4 that, the whole plant N–P–S concentration correlated significantly and negatively with canopy spectral reflectance in the VIS region and positively in NIR region. The correlation of S with the spectral reflectance was negative and significant in 660–680 nm section of the VIS region. Interesting to notice that, the whole plant N and P

concentration correlated significantly with the spectral reflectance in the SWIR region. But, the values of correlation coefficient were lower than those observed in the VIS and NIR region. Sudden drop in the value of correlation coefficient from 1092 nm onwards to 1150 nm was observed for N, P and S but it was more conspicuous for S (Fig. 5). This could be due to the absorption feature of canopy water content. The correlation coefficient for N and P were the highest and most significant at 1460 nm in the SWIR region. On the contrary to leaf reflectance, the pattern of N, P and S correlation with the spectral reflectance at canopy level was similar over the entire wavelength region. The different wavelengths selected from linear correlation analysis are linked to the physical properties as: (1) 670 nm—near to electron transition in chlorophyll *a* and *b* (Osborne et al. 1993; Curran, 1989; Zur et al. 2000) (2) 700 nm—pigments present in the foliage (Ecartot et al. 2013) (or the cell structure, however specific cause is unknown in the present study) and (3) 730, 1090, 1092 and 1260 nm—change in cell structure alter the internal scattering at air-cell water interfaces within the leaves (Thomas and Oerther, 1972) and (4) 1460 nm—near absorption feature of protein nitrogen (N–H bond) (1510 nm) (Curran 1989; Hermann et al. 2010) (Fig. 6).

### Vegetation indices

The dynamic change pattern of the hyperspectral reflectance to variable N–P–S concentration proposes a basis to process radiometric data to construct spectral algorithms for quantitative retrieval of N–P–S in rice plants. Spectral algorithms for quantitative retrieval of N in rice are available in recently published literature.

Using the results of linear correlation analysis, new VIs were proposed for P and S prediction. These indices includes P (670, 1092, 1260 and 1460 nm) and S (670 and 1090 nm) sensitive wavelengths. New VIs proposed are based on the outcomes of correlation analysis between canopy spectral reflectance and the whole plant N–P–S concentration for wide scale applicability at field level. In the SWIR region, N and P correlations were higher and significant at 1460 nm ( $r = 0.33$ ,  $p < 0.05$ ). These finding are concordant with those by Pimstein et al. (2011) and could be the potential zone to develop new spectral

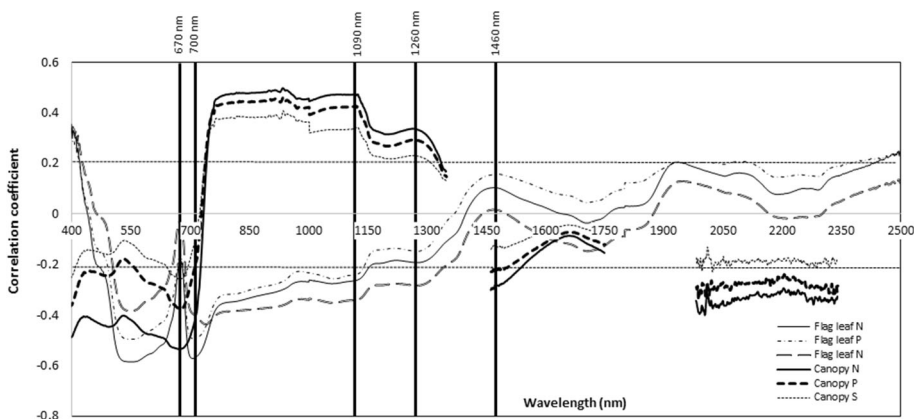


**Fig. 6** Linear correlation between the flag leaf and canopy N–P–S concentrations and the hyperspectral reflectance. A dotted line parallel to x-axis represents significance of correlation coefficient at 5% level. Vertical lines indicated with wavelengths shows the wavelengths with the highest correlation coefficient for N, P and S

algorithms to discriminate N and P stress. They reported a significant correlation of N-P-K concentration with the spectral reflectance at 1450 nm. The highest correlation was observed for K, which was followed by N and it was lowest for P. Wavelength 1460 nm is very close to water absorption bands, so the spectral reflectance could be affected by atmospheric moisture. In the present investigation, wavelength 1460 nm has been used for proposing new VIs. While using such wavelengths for nutrient stress differentiation, special care was taken to omit the water absorption bands which would otherwise have led to erroneous results.

Three new VIs for P (Eq. 4–6) and one for S (Eq. 7) monitoring were proposed in the present study. All three VIs were proposed as normalized configuration in order to enhance differences and obtain positive values (Pimstein et al. 2011).

The nomenclature pattern of the VIs was adopted from Pimstein et al. (2011) and Mahajan et al. (2014) to make the indices self-explanatory.

$$P_{670\_1260} = \frac{(R_{1260} - R_{670})}{(R_{1260} + R_{670})} \quad (5)$$

$$P_{1092\_1260} = \frac{(R_{1092} - R_{1260})}{(R_{1092} + R_{1260})} \quad (6)$$

$$P_{1260\_1460} = \frac{(R_{1260} - R_{1460})}{(R_{1260} + R_{1460})} \quad (7)$$

$$S_{670\_1090} = \frac{(R_{1090} - R_{670})}{(R_{1090} + R_{670})} \quad (8)$$

R, represents the hyperspectral reflectance at the subscripted wavelength.

### Nutrient prediction using vegetation indices

To estimate capability and reliability of the VIs to predict nutrient concentration in the whole plant, model of VIs were developed using one year dataset were cross validated on another year dataset. Moreover, performance of multi-year model was also tested on the single year dataset. The model parameters RMSE, RE and RPD were used to test precision of model and agreement between actual and predicted values of nutrient concentration. Comparison between RMSE, RE and RPD were made to identify VI to monitor macronutrient concentration in rice plants.

### Prediction of nitrogen

The results of cross-validation of already published and newly proposed VIs models for N prediction is presented in Table 4. Only four VIs viz. NDVI broadband, NDVI hyper, GNDVI and  $NRI_{1510}$  among seven tested published VIs could predict N concentration significantly for 2010-to-2011 and 2011-to-2010 cross validation. Accuracy of prediction for single-year model for these three VIs was found to be  $r = 0.42\text{--}0.62$  ( $p < 0.01$ ),  $RMSE = 0.301\text{--}0.436\%$ ,  $RE = 7.82\text{--}12.16\%$  and  $RPD = 2.13\text{--}3.01$ . When single-year model of four newly proposed VIs were cross-validated on other years data, the model could predict N concentration significantly with accuracy of prediction as  $r = 0.43\text{--}0.60$  ( $p < 0.01$ ),  $RMSE = 0.332\text{--}0.426\%$ ,  $RE = 9.32\text{--}13.46\%$  and  $RPD = 1.67\text{--}2.93$ . This reflects the higher precision of the already existing traditional VIs for N monitoring in crops.



**Table 4** Relationship between actual (laboratory analyzed) and predicted (using regressive models of vegetation indices) rice canopy N content

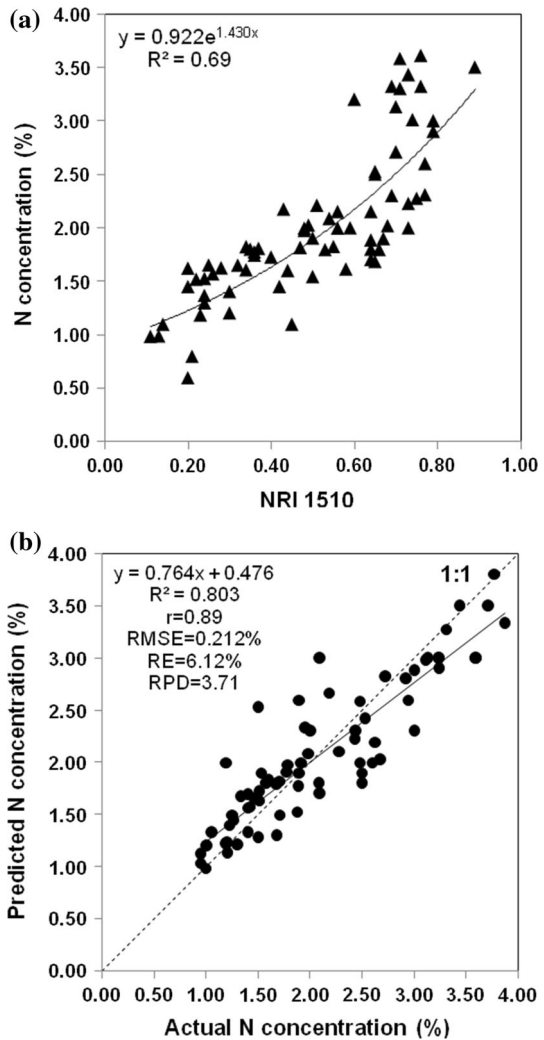
	r	RMSE (%)	RE (%)	RPD
2010-to-2011 cross validation [calibration dataset—2010 (n = 72); validation dataset—2011 (n = 72)]				
NDVI broadbands	0.62 ( $p < 0.01$ )	0.301	7.82	3.01
NDVI hyper	0.61 ( $p < 0.01$ )	0.366	9.61	2.21
GNDVI	0.42 ( $p < 0.01$ )	0.432	9.82	2.13
SAVI	ns	ns	ns	ns
OSAVI	ns	ns	ns	ns
NRI <sub>1510</sub>	0.81 ( $p < 0.01$ )	0.212	6.12	3.71
N_1645_1715	ns	ns	ns	ns
P_670_1260	0.59 ( $p < 0.01$ )	0.401	10.12	1.96
P_1092_1460	0.49 ( $p < 0.01$ )	0.413	12.37	1.82
P_1260_1460	0.52 ( $p < 0.01$ )	0.391	13.46	1.73
S_670_1090	0.60 ( $p < 0.01$ )	0.332	9.32	2.88
2011-to-2010 cross validation [calibration dataset—2011 (n = 72); validation dataset—2010 (n = 72)]				
NDVI broadbands	0.58 ( $p < 0.01$ )	0.412	10.12	2.83
NDVI hyper	0.62 ( $p < 0.01$ )	0.401	11.32	2.31
GNDVI	0.47 ( $p < 0.01$ )	0.436	12.16	2.88
SAVI	ns	ns	ns	ns
OSAVI	ns	ns	ns	ns
NRI <sub>1510</sub>	0.71 ( $p < 0.01$ )	0.328	9.74	2.92
N_1645_1715	ns	ns	ns	ns
P_670_1260	0.56 ( $p < 0.01$ )	0.392	11.13	1.96
P_1092_1460	0.43 ( $p < 0.01$ )	0.426	12.01	1.67
P_1260_1460	0.46 ( $p < 0.01$ )	0.419	12.39	2.03
S_670_1090	0.59 ( $p < 0.01$ )	0.397	10.32	2.93

*r* correlation coefficient, *RMSE* root means square error of prediction, *RE* relative error, *RPD* ratio of performance to deviation

Among all combinations, prediction accuracy of 2010-to-2011 cross-validation of NRI<sub>1510</sub> model was the highest. A significant exponential relationship between NRI<sub>1510</sub> and N concentration was obtained for the 2010 calibration model (Fig. 7a). A close agreement was observed between actual laboratory analysed and predicted N concentration in 1:1 scatter diagram (Fig. 7b). The accuracy of prediction for the NRI<sub>1510</sub> VI model was found to be  $r = 0.89$  ( $p < 0.01$ ),  $RMSE = 0.212\%$ ,  $RE = 6.12\%$  and  $RPD = 3.71$ . These findings are concordant with those by Herrmann et al. (2010), they formulated SWIR based VI for monitoring the N status of potato. They found NRI<sub>1510</sub> as robust VI with prediction accuracy  $R^2 = 0.59$  ( $p < 0.005$ ) and  $RMSE = 0.421\%$ . The NRI<sub>1510</sub> has advantages since it is directly related to N content (by 1510 nm) and indirectly related to N by chlorophyll (by 660 nm) while other indices are usually only indirectly related to N.

Recent literature reports different simple ratios, normalized configurations, absolute reflectance, first and second order derivatives of reflectance, specific narrow-band (two, three, etc.) VIs in different crops. The popular and traditional VIs were evaluated for rice N

**Fig. 7 a** Exponential calibration model of  $NRI_{1510}$  and N concentration using the dataset 2010 and **b** actual versus predicted N canopy concentration (prediction accuracy as  $R^2 = 0.80$ ,  $r = 0.89$ ,  $RMSE = 0.212\%$ ,  $RE = 6.12\%$  and  $RPD = 3.71$ ) using  $NRI_{1510}$  calibration model 2010 validated on 2011 dataset



prediction in the present study to investigate their P and S predictability along with N. To make macronutrient prediction simpler, simple VIs were designed using two highly sensitive and nutrient specific wavelengths for each of the nutrients. Such wavelengths can be used to design handheld tools (like chlorophyll meters) to estimate macronutrient status of crop plants in real time. Four such VIs for P and one for S prediction were proposed in the present investigation.

### Prediction of phosphorus

Cross-validation results of models of the VIs for P prediction were presented in Table 5. The 2010-to-2011 cross validation revealed the poor predictive ability of published VIs except recently published  $N_{1645\_1715}$ . Prediction accuracy of this cross-validation using  $N_{1645\_1715}$  model was  $r = 0.51$  ( $p < 0.01$ ),  $RMSE = 0.031\%$ ,  $RE = 12.73\%$  and

**Table 5** Relationship between actual (laboratory analyzed) and predicted (using regressive models of vegetation indices) rice canopy P content

	r	RMSE (%)	RE (%)	RPD
2010-to-2011 cross validation [calibration dataset—2010 (n = 72); validation dataset—2011 (n = 72)]				
NDVI broadbands	0.31 ( $p < 0.05$ )	0.047	13.87	2.11
NDVI hyper	0.33 ( $p < 0.01$ )	0.045	13.19	1.93
GNDVI	ns	ns	ns	ns
SAVI	ns	ns	ns	ns
OSAVI	ns	ns	ns	ns
NRI <sub>1510</sub>	0.38 ( $p < 0.01$ )	0.041	13.01	1.99
N_1645_1715	0.51 ( $p < 0.01$ )	0.031	12.73	2.78
P_670_1260	0.53 ( $p < 0.01$ )	0.028	10.21	2.99
P_1092_1460	0.49 ( $p < 0.01$ )	0.030	10.30	2.86
P_1260_1460	0.50 ( $p < 0.01$ )	0.031	10.67	2.94
S_670_1090	0.41 ( $p < 0.01$ )	0.034	11.48	2.52
2011-to-2010 cross validation [calibration dataset—2011 (n = 72); validation dataset—2010 (n = 72)]				
NDVI broadbands	0.34 ( $p < 0.01$ )	0.042	12.26	2.17
NDVI hyper	0.36 ( $p < 0.01$ )	0.040	14.21	1.96
GNDVI	0.29 ( $p < 0.05$ )	0.045	13.01	1.63
SAVI	ns	ns	ns	ns
OSAVI	ns	ns	ns	ns
NRI <sub>1510</sub>	0.41 ( $p < 0.01$ )	0.030	11.93	2.74
N_1645_1715	0.55 ( $p < 0.01$ )	0.029	10.17	3.01
P_670_1260	0.67 ( $p < 0.01$ )	0.023	9.12	3.68
P_1092_1460	0.63 ( $p < 0.01$ )	0.024	9.66	3.59
P_1260_1460	0.65 ( $p < 0.01$ )	0.026	9.82	3.32
S_670_1090	0.44 ( $p < 0.01$ )	0.027	10.96	2.89

*r* correlation coefficient, *RMSE* root means square error of prediction, *RE* relative error, *RPD* ratio of performance to deviation

RPD = 2.78. Although P prediction using NDVI broadbands and NDVI hyper were statistically significant, it does not provide enough levels of accuracy of prediction ( $r \geq 0.33$  ( $p < 0.01$ ),  $RMSE \geq 0.045\%$ ,  $RE \geq 13.19\%$  and  $RPD \leq 2.11$ ). However, it is interesting to note that, the P characterizing ability of newly proposed P dedicated VIs reached acceptable levels of accuracies. Relatively lower error in predicting the rice plant P concentration was obtained for 2010-to-2011 cross validation of VIs model of three newly proposed VIs ( $RMSE \leq 0.031\%$ ,  $RE \leq 10.67\%$ ,  $RPD \geq 2.86$ ). The significantly ( $p < 0.05$ ) highest predictions were observed for P\_670\_1260 with prediction accuracy as  $r = 0.53$  ( $p < 0.01$ )  $RMSE = 0.028\%$ ,  $RE = 10.21\%$  and  $RPD = 2.99$ . Though, NRI<sub>1510</sub> is a dedicated VI for N monitoring, the research results revealed that the prediction of P using the VI was significant [ $r = 0.38$  ( $p < 0.01$ ),  $RMSE = 0.041\%$ ,  $RE = 13.01\%$  and  $RPD = 1.99$ ].

Similar sort of trend was observed for 2011-to-2010 cross validation. Although, P concentration using traditional VIs NDVI broadbands, NDVI hyper and GNDVI were

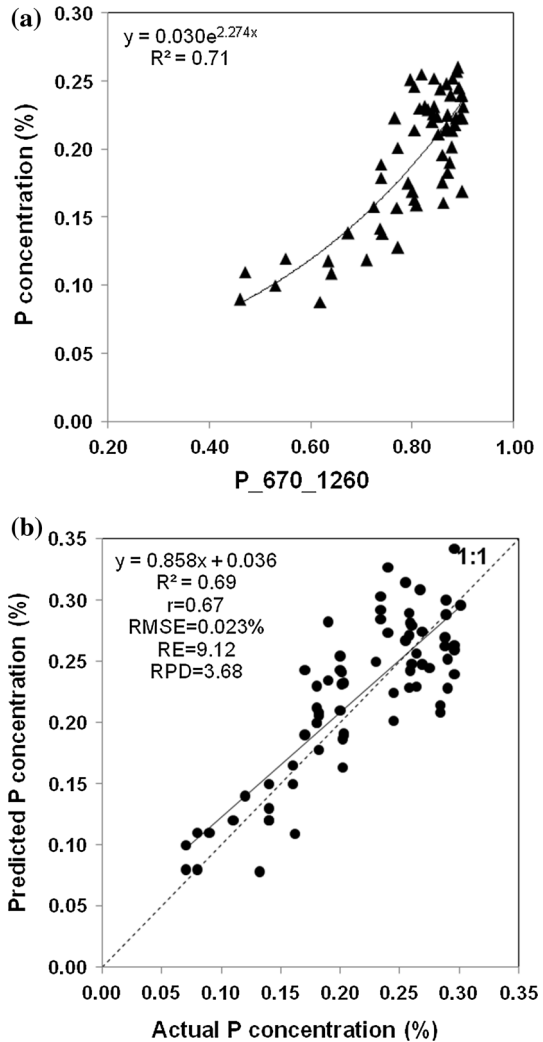
statistically significant, but resulted in high errors in predictions (RMSE = 0.040%, RE = 12.26–14.21% and RPD = 1.63–2.17). When newly proposed P dedicated VIs P\_670\_1260, P\_1092\_1460 and P\_1260\_1460 models of 2011 were tested on P status of 2010, significantly ( $p < 0.05$ ) higher predictions with minimum error ( $r = 0.63$ – $0.67$  ( $p < 0.01$ ), RMSE = 0.023–0.029%, RE = 9.12–9.82% and RPD = 3.32–3.68) were obtained. These predictions correspond to an excellent screening of predictive models of VIs. Among these three VIs, P\_670\_1260 was able to predict P concentration in rice more correctly with higher correlation and relatively lower error. Like the 2010-to-2011 cross validation, the P prediction accuracy of the NRI<sub>1510</sub> was significant with  $r = 0.41$  ( $p < 0.01$ ), RMSE = 0.030%, RE = 11.93% and RPD = 2.74. It is noticeable here that, there is a potential of using the VIS-SWIR based VI, NRI<sub>1510</sub>, for monitoring P in rice plants as well. However, the results in the present study might be attributed to the significant correlation ( $r \geq 0.68$  in the flag leaf and  $r \geq 0.48$  in the canopy,  $p < 0.05$ ) between the N and P in the flag leaf and canopy. It is very interesting to see that, prediction accuracies of all VIs were found to be significantly improved for 2011-to-2010 cross validation (Table 5). Improvement in predictive ability of 2011-to-2010 over 2010-to-2011 cross validation may be attributed to higher variability in P concentration in 2011. The P concentration variability in 2011 was 1.66 times that in 2010, making 2011 dataset more suitable for developing P prediction models.

The calibration model of 2011 ( $R^2 = 0.71$ ,  $p < 0.01$ ) i.e. an exponential relationship between P\_670\_1260 and P concentration (Fig. 8a) cross validated on 2010 appeared most robust in retrieving P concentration in rice plants. A linear response, steep slope and uniformly scattered values of predicted P concentration against actual and laboratory analyzed concentration around 1:1 scatter line depicts robustness of P\_670\_1260 to quantify plant P status (Fig. 8b). Accurate predictions of single year models of P\_670\_1260 are due to the inclusion of wavelengths in the VIS (670 nm) and NIR (1260 nm) which showed significant correlations with P concentration (Fig. 6). The use of wavelengths in the VIS and NIR region for P retrieval has been successfully demonstrated in corn crop (Osborne et al. 2002) and wheat (Ayala-Silva and Beyl 2005) using different statistical analytical methods. And these reports support the use of VIS–NIR based VI P\_670\_1260 for P retrieval in rice. Earlier work reported by Pimstein et al. (2011) on VI N\_1645\_1715 based P retrieval in the wheat canopy are in agreement with significant P prediction in using the same in the present investigation. They reported use of N\_1645\_1715 relatively advantageous because wavelengths located out of water absorption regions and their inclusion in spectral bands of airborne hyperspectral images. Cross-validation of N\_1645\_1715 model was found to have acceptable levels of accuracies ( $r = 0.51$ – $0.55$  ( $p < 0.01$ ), RMSE = 0.029–0.036%, RE = 10.02–12.73% and RPD = 2.78–3.01). So, VI N\_1645\_1715 can also be used in rice crop to quantify canopy P in rice as well along with newly proposed VIs. In future, the use of wavelengths in the SWIR (1645 and 1715 nm), VIS (670 nm) and NIR (1260 nm) can be evaluated to achieve higher P prediction accuracies in different crops.

## Prediction of sulphur

Table 6 shows cross-validation results of models of the traditional VIs as well as newly proposed VIs. Three VIs (NDVI broadband, NDVI hyper and GNDVI) among six published could significantly predict S concentration for 2010-to-2011 cross validation combination. But, the levels of accuracies ( $r = 0.28$ – $0.31$  ( $p < 0.01$ ), RMSE = 0.039–0.042%, RE = 15.18–17.29% and RPD = 1.62–1.98) were not enough and acceptable. The

**Fig. 8 a** Exponential calibration model of P<sub>670\_1260</sub> and P concentration using the dataset 2011 and **b** actual versus predicted P canopy concentration in rice (prediction accuracy as  $R^2 = 0.69$ ,  $r = 0.67$ ,  $RMSE = 0.023\%$ ,  $RE = 9.12\%$  and  $RPD = 3.68$ ) using P<sub>670\_1260</sub> calibration model 2011 validated on 2010 dataset



strongest results were obtained using a model of S dedicated VI S<sub>670\_1090</sub> with prediction accuracy of  $r = 0.52$  ( $p < 0.01$ ),  $RMSE = 0.021\%$ ,  $RE = 10.11\%$  and  $RPD = 2.87$ . For this cross-validation combination, screening VI model of S<sub>670\_1090</sub> was satisfactory. The  $NRI_{1510}$  predicted the S concentration with a significant prediction accuracy of  $r = 0.48$  ( $p < 0.01$ ),  $RMSE = 0.023\%$ ,  $RE = 10.98\%$  and  $RPD = 2.41$ , it was lesser compared to the newly proposed VIs but higher than the published ones. The positive correlation ( $r \geq 0.66$  in flag leaf and  $r \geq 0.59$  in the canopy,  $p < 0.05$ ) between N and S could possibly a reason for significant S prediction using the  $NRI_{1510}$ . Similar sort of trend of cross-validation results was observed for 2011-to-2010 cross validation. The NDVI broadbands, NDVI hyper and GNDVI showed prediction accuracy of  $r = 0.33$ – $0.37$  ( $p < 0.01$ ),  $RMSE = 0.032$ – $0.037\%$ ,  $RE = 11.27$ – $13.12\%$  and  $RPD = 1.75$ . Prediction accuracy ( $r = 0.62$  ( $p < 0.01$ ),  $RMSE = 0.018\%$ ,  $RE = 9.87\%$  and  $RPD = 3.17$ ) using S<sub>670\_1090</sub> model was highest among different cross validation combinations. An

**Table 6** Relationship between actual (laboratory analyzed) and predicted (using regressive models of vegetation indices) rice canopy S content

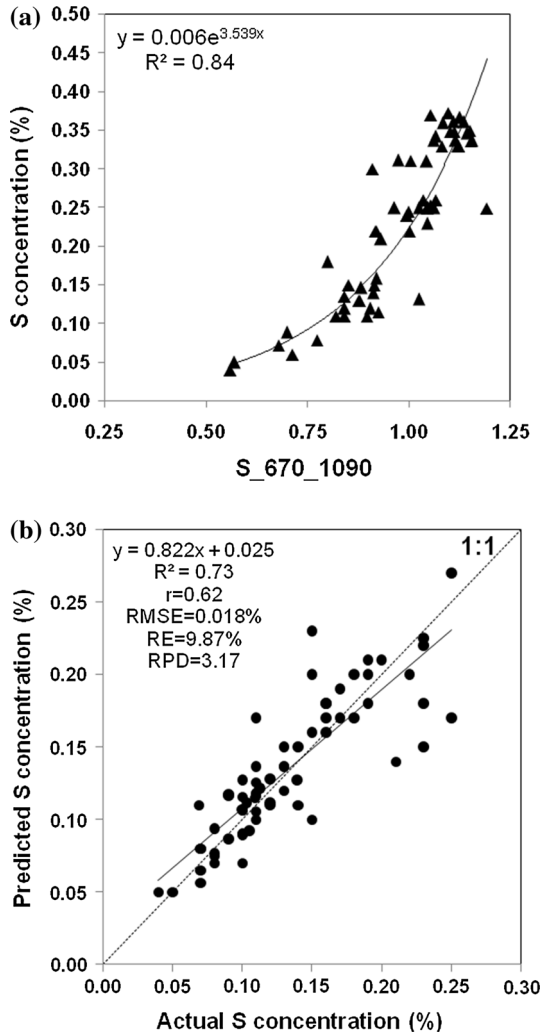
	r	RMSE (%)	RE (%)	RPD
2010-to-2011 cross validation [calibration dataset—2010 (n = 72); validation dataset—2011 (n = 72)]				
NDVI broadbands	0.31 ( $p < 0.05$ )	0.042	16.71	1.91
NDVI hyper	0.28 ( $p < 0.05$ )	0.041	15.18	1.78
GNDVI	0.29 ( $p < 0.05$ )	0.039	17.29	1.62
SAVI	ns	ns	ns	ns
OSAVI	ns	ns	ns	ns
NRI <sub>1510</sub>	0.48 ( $p < 0.01$ )	0.023	10.98	2.41
N_1645_1715	ns	ns	ns	ns
P_670_1260	0.50 ( $p < 0.01$ )	0.021	10.21	2.54
P_1092_1460	0.33 ( $p < 0.01$ )	0.033	12.36	2.09
P_1260_1460	ns	ns	ns	ns
S_670_1090	0.52 ( $p < 0.01$ )	0.021	10.11	2.87
2011-to-2010 cross validation [calibration dataset—2011 (n = 72); validation dataset—2010 (n = 72)]				
NDVI broadbands	0.37 ( $p < 0.01$ )	0.032	11.27	2.01
NDVI hyper	0.33 ( $p < 0.01$ )	0.034	12.68	1.85
GNDVI	0.33 ( $p < 0.01$ )	0.037	13.12	1.72
SAVI	ns	ns	ns	ns
OSAVI	ns	ns	ns	ns
NRI <sub>1510</sub>	0.54 ( $p < 0.01$ )	0.028	10.84	2.64
N_1645_1715	ns	ns	ns	ns
P_670_1260	0.58 ( $p < 0.01$ )	0.024	10.07	2.92
P_1092_1460	0.42 ( $p < 0.01$ )	0.037	12.82	2.15
P_1260_1460	ns	ns	ns	ns
S_670_1090	0.62 ( $p < 0.01$ )	0.018	9.87	3.17

r correlation coefficient, RMSE root means square error of prediction, RE relative error, RPD ratio of performance to deviation

exponential relationship between S\_670\_1090 and S concentration ( $R^2 = 0.84$ ,  $p < 0.01$ ) was the robust among all the calibration models for S (Fig. 9a). The close agreement between actual and predicted values and their uniform spread along 1:1 scatter line explains robustness of S\_670\_1090 model for retrieving S concentration (Fig. 9b). A possible reason for improvement in S characterizing ability of 2011-to-2010 dataset may be higher reliability in S concentration in 2011. The CV for S concentration in 2011 dataset was 1.30 times higher than 2010 dataset. Higher correlation with a relatively lower error made 2011 model suitable for retrieving S concentration in rice.

It is important to notice a little difference between prediction accuracies using S\_670\_1090 and P\_670\_1260 model for all cross-validation results. If we critically analyze the structure of both of these VIs then it is clear that they include one common wavelength 670 nm in the VIS and one for both which lies in the NIR region. Higher sensitivity of the spectral reflectance at 1090 nm than 1260 nm with S concentration (Fig. 4) explains comparatively higher prediction accuracy using S\_670-1090 model. Lack of sensitivity of N\_1645\_1715 for S retrieval is noticeable in Table 6. One major reason

**Fig. 9 a** Exponential calibration model of P\_670\_1090 and P concentration using the dataset 2011 and **b** actual versus predicted S canopy concentration in rice (prediction accuracy as  $R^2 = 0.73$ ,  $r = 0.62$ ,  $RMSE = 0.018\%$ ,  $RE = 9.87\%$  and  $RPD = 3.17$ ) using P\_670\_1090 calibration model 2011 validated on 2010 dataset



for obtained results may be insignificant correlation of the spectral reflectance at wavelengths 1645 and 1715 nm with S concentration both in lab as well as canopy (Fig. 4). The probable reasons for obtaining the best results during the cross validations could be higher variability created in plant N, P and S concentration, proper grouping of observation for the calibration and validation dataset and selection of appropriate wavelengths specific to the nutrient concentration.

Considering the complexity and requirement of huge information on number of wavelengths, spectral algorithms based on few nutrient sensitive wavelengths may prove useful for remote N, P and S prediction. We envisage that such algorithms could be used for designing sensors of handheld instruments for macronutrient prediction of canopy (e.g. chlorophyll meter for relative N estimation). The use of satellite remote sensing applications is becoming increasingly popular because (1) spectral bandwidth has decreased dramatically with the advent of hyperspectral remote sensing, (2) variety of spectral

indices have been developed for agricultural applications rather than only the normalized difference vegetation indices, (3) improvement of spatial resolution of remote sensing satellites with 100s of meter to sub-meter accuracy (e.g. World View-2 (launched in the year 2009) with spectral bands—P, B, G, Y, R, red edge and NIR and spatial resolution of 0.5 m) and (4) improved temporal frequency of remote sensing satellites (Mulla 2013). Retrieval of broadband data using multispectral sensors often loses critical information on specific narrow bands (Blackburn 1998). Hyperspectral remote sensing acquires images in many narrow and contiguous spectral bands, thus provides a continuous spectrum for each pixel, unlike multi-spectral systems that acquires images in few broad spectral bands (Hansen and Schjoerring 2003). The approach of remote sensing research for crop nutrient monitoring in future should be towards developing simple algorithms, simple procedure and simple and cheaper devices with major focus on end users and farmers. This study elucidates a new knowledge on the P and S monitoring in hybrid rice using remote sensing as the information on this aspect in rice or other crops is little known. The output of the present study can be utilized for site specific and real time management of N, P and S in hybrid rice. To achieve this, the rapidly-expanding availability of the small drone to capture spectral data of interest (e.g. wavelengths proposed in the study) can be very much useful.

## Conclusions

The results of the study demonstrated that the radiometric data could be used for prediction and monitoring of N, P and S status in the rice crop at the panicle initiation stage. Linear correlation analysis of N–P–S concentration with reflectance showed the presence of significantly sensitive wavelengths in the energy spectrum. Few N–P–S sensitive wavelengths—670, 700, 730, 1090, 1260, 1460 nm etc. along the energy spectrum were observed at the flag leaf and canopy level. The N predictions were significantly ( $p < 0.05$ ) achieved using the VIS and SWIR based VI  $NRI_{1510}$ . Out of newly proposed VIs  $P_{670\_1092}$  and  $P_{670\_1260}$  for P and  $S_{670\_1090}$  for S prediction were found to be most robust with higher prediction accuracies using their regressive models.

**Acknowledgements** The award of a Senior Research Fellowship by the Indian Council of Agricultural Research, New Delhi, to Mahajan G. R. and Institutional support from Indian Agricultural Research Institute, New Delhi, India is gratefully acknowledged. Authors are especially thankful to Division of Agricultural Physics, Indian Agricultural Research Institute, New Delhi, India for providing the spectroradiometer for carrying out the present research work. The experimental set up designed under the All India Coordinated Research Project (ICAR—Indian Institute of Soil Science) is gratefully acknowledged.

## References

- Ayala-Silva, T., & Beyl, C. A. (2005). Changes in spectral reflectance of wheat leaves in response to specific macronutrient deficiency. *Advances in Space Research*, 35, 305–317.
- Basayigit, L., & Senol, H. (2009). Prediction of plant nutrient contents in deciduous orchards fruits using spectroradiometer. *International Journal of Chem Tech Research*, 1, 212–224.
- Blackburn, G. A. (1998). Quantifying chlorophylls and carotenoids at leaf and canopy scales: An evaluation of some hyperspectral approaches. *Remote Sensing of Environment*, 66, 273–285.
- Chen, S., Li, D., Wang, Y., Zhiping, P., & Chen, W. (2011). Spectral characterization and prediction of nutrient content in winter leaves of litchi during flower bud differentiation in southern China. *Precision Agriculture*, 12, 682–698.



- Crookston, K. (2006). A top 10 list of developments and issues impacting crop management and ecology during the past 50 years. *Crop Science*, *46*, 2253–2262.
- Curran, P. J. (1989). Remote sensing of foliar chemistry. *Remote Sensing of Environment*, *30*, 271–278.
- Ecartot, M., Compan, F., & Roumet, P. (2013). Assessing leaf nitrogen content and leaf mass per unit area of wheat in the field throughout plant cycle with a portable spectrometer. *Field Crops Research*, *140*, 44–50.
- Feng, W., Yao, X., Zhu, Y., Tian, Y. C., & Cao, W. (2008). Monitoring leaf nitrogen status with hyperspectral reflectance in wheat. *European Journal of Agronomy*, *28*, 394–404.
- Gitelson, A., Kaufman, Y., & Merzlyak, M. (1996). Use of a green channel in remote sensing of global vegetation from EOS-MODIS. *Remote Sensing of Environment*, *58*, 289–298.
- Gomez-Casero, M. T., Lopez-Granados, F., Pena-Barragan, J. M., Jurado-Exposito, M., Garcia-Torres, L., & Fernandez-Escobar, R. (2007). Assessing nitrogen and potassium deficiencies in olive orchards through discriminant analysis of hyperspectral data. *Journal of American Society of Horticultural Sciences*, *132*, 611–618.
- Hansen, P. M., & Schjoerring, J. K. (2003). Reflectance measurement of canopy biomass and nitrogen status in wheat crops using normalized difference vegetation indices and partial least squares regression. *Remote Sensing of Environment*, *86*, 542–553.
- Hanway, J. J., & Heidel, H. (1952). Soil analysis methods as used in Iowa State College Soil Testing Laboratory. *Bulletin*, *57*, 1–31.
- Henao, J., & Baanate, C. (1999). Estimating rates of nutrient depletion in soils of agricultural land of Africa. Technical Bulletin IFDC-T-48, pp. 1–76.
- Herrmann, I., Karnieli, A., Bonfil, D. J., Cohen, Y., & Alchanatis, V. (2010). SWIR-based spectral indices for assessing nitrogen content in potato fields. *International Journal of Remote Sensing*, *31*, 5127–5143.
- Huete, A. (1988). A soil-adjusted vegetation index (SAVI). *Remote Sensing of Environment*, *25*, 295–309.
- Inoue, Y. (2003). Synergy of remote sensing and modeling for estimating ecophysiological processes in plant production. *Plant Production Science*, *6*, 3–16.
- Inoue, Y., & Penuelas, J. (2001). An AOTF-based hyperspectral imaging system for field use in ecophysiological and agricultural applications. *International Journal of Remote Sensing*, *22*, 3883–3888.
- Institute, S. A. S. (2012). *SAS User's guide*. IC, Cary: SAS Institute.
- Jackson, M. L. (1973). *Soil Chemical Analysis*. New Delhi: Prentice Hall of India Private Limited press.
- Jamieson, P. D., Porter, J. R., & Wilson, D. R. (1991). A test of the computer simulation model ARC-WHEAT1 on wheat crops grown in New Zealand. *Field Crop Research*, *27*, 337–350.
- Jorgensen, R. N., Christensen, L. K., & Bro, R. (2007). Spectral reflectance at sub-leaf scale including the spatial distribution discriminating NPK stress characteristics in barley using multi-way partial least squares regression. *International Journal of Remote Sensing*, *28*, 943–962.
- Knox, N. M., Skidmore, A. K., Prins, H. H. T., Heitkonig, I. M. A., Slotow, R., Waal, C. V. D., et al. (2012). Remote sensing of forage nutrients: Combining ecological and spectral absorption feature data. *ISPRS Journal of Photogrammetry and Remote Sensing*, *72*, 27–35.
- Lesschen, J. P., Asiamah, R. D., Gicheru, P., Kanté, S., Stoorvogel, J. J., & Smaling, E. M. A. (2003). *Scaling soil nutrient balances*. Rome: FAO.
- Lindsay, W. L., & Norvell, W. A. (1978). Development of a DTPA test for zinc, iron, manganese and copper. *Soil Science Society of America Journal*, *42*, 421–428.
- Mahajan, G. R., Sahoo, R. N., Pandey, R. N., Gupta, V. K., & Kumar, D. (2014). Using hyperspectral remote sensing techniques to monitor nitrogen, phosphorus, sulphur, potassium in wheat (*Triticum aestivum*). *Precision Agriculture*, *15*, 499–522.
- Malley, D. F., Lockhart, L., Wilkinson, P., & Hauser, B. (2000). Determination of carbon, nitrogen, and phosphorus in freshwater sediments by near infrared reflectance spectroscopy: Rapid analysis and a check on conventional analytical methods. *Journal of Paleolimnology*, *24*, 415–425.
- Mulla, D. J. (2013). Twenty-five years of remote sensing in precision agriculture: Key advances and remaining knowledge gaps. *Biosystem Engineering*, *114*, 358–371.
- Olsen, S. R., Cole, C. V., Watanabe, F. S., & Dean, L. (1954). Estimation of available phosphorus in soils by extraction with sodium bicarbonate. USDA Circ. 93. Washington: US Govt. Printing Office.
- Osborne, B. G., Fearn, T., & Hindle, P. H. (1993). *Practical NIR spectroscopy with applications in food and beverage analysis* (pp. 36–40). Harlow/New York: Longman Scientific and Technical/Wiley.
- Osborne, S., Schepers, J., Francis, D., & Schlemmer, M. (2002). Detection of phosphorus and nitrogen deficiencies in corn using spectral radiance measurements. *Agronomy Journal*, *94*(6), 1215–1221.
- Pimstein, A., Karnieli, A., Bansal, S. K., & Bonfil, D. J. (2011). Exploring remotely sensed technologies for monitoring wheat potassium and phosphorus using field spectroscopy. *Field Crop Research*, *121*, 125–135.

- Prabhakar, M., Prasad, Y. G., Thirupathi, M., Sreedevi, G., Dharajothi, B., & Venkateswarlu, B. (2011). Use of ground based hyperspectral remote sensing for detection of stress in cotton caused by leafhopper (*Hemiptera: Cicadellidae*). *Computer and Electronics in Agriculture*, 79, 189–198.
- Ramamoorthy, B., Narasimhan, R. L., & Dinesh, R. S. (1967). Fertilizer application for specific yield targets on Sonora 64 (wheat). *Indian Farming*, 17, 43–45.
- Ramoelo, A., Skidmore, A. K., Chao, M. A., Mathieu, R., Heitkong, I. M. A., Dudeni-Tihone, N., et al. (2013). Non-linear partial least square regression increases the estimation accuracy of grass nitrogen and phosphorus using in situ hyperspectral and environmental data. *ISPRS Journal of Photogrammetry and Remote Sensing*, 72, 27–35.
- Ranjan, R., Chopra, U. K., Sahoo, R. N., Singh, A. K., & Pradhan, S. (2012). Assessment of plant nitrogen stress in jwheat (*Triticumaestivum* L.) through hyperspectral indices. *International Journal of Remote Sensing*, 33, 6342–6360.
- Rondeaux, G., Steven, M., & Baret, F. (1996). Optimization of soil-adjusted vegetation indices. *Remote Sensing of Environment*, 55, 95–107.
- Rouse, J., Haas, R. H., Schell, J. A., & Deering, D. W. (1974). Monitoring vegetation systems in the Great Plains with ERTS. In 3rd Earth Resources Technology Satellite-1 symposium, NASA SP-351, Greenbelt (pp. 301–317).
- Ryu, C. S., Suguri, M., & Umeda, M. (2009). Model for predicting the nitrogen content of rice at panicle initiation stage using data from airborne hyperspectral remote sensing. *Biosystem Engineering*, 104, 465–475.
- Sheldrick, W. F., Syers, J. K., & Lingard, J. (2003). Soil nutrient audits for China to estimate nutrient balances and output/input relationships. *Agricultural Ecosystems and Environment*, 94, 341–354.
- Steven, M. C. (2004). Correcting the effects of field of view and varying illumination in spectral measurements of crops. *Precision Agriculture*, 5, 55–72.
- Stoorvogel, J. J., & Smaling, E. M. A. (1990). Assessment of soil nutrient depletion in sub-Saharan Africa: 1983–2000. Report 28. Wageningen: Winand Staring Centre.
- Stroppiana, D., Boschetti, M., Brivio, P. A., & Bocchi, S. (2009). Plant nitrogen concentration in paddy rice from field canopy hyperspectral radiometry. *Field Crop Research*, 11, 119–129.
- Subbiah, B. V., & Asija, G. L. (1956). A rapid procedure for the estimation of available Nitrogen in soil. *Current Science*, 25, 259–260.
- Tabatabai, M. A., & Bremer, J. M. (1970). A simple turbidimetric method of determining total sulphur in plant materials. *Agronomy Journal*, 62, 805–806.
- Tan, Z. X., Lal, R., & Wiebe, K. D. (2005). Global soil nutrient depletion and yield reduction. *Journal of Sustainable Agriculture*, 26, 123–146.
- Tandon, H. L. S. (2004). *Fertilizers in Indian agriculture—From 20th to 21st century*. New Delhi: FDCO.
- Thomas, J. R., & Oerther, G. F. (1972). Estimating nitrogen content of sweet pepper leaves by reflectance measurements. *Agronomy Journal*, 64, 11–13.
- Walkley, A. J., & Black, I. A. (1934). An estimation of the Degtjareff method for determining soil organic matter and a proposed modification of the chromic acid titration method. *Soil Science*, 37, 29–38.
- Williams, P., & Norris, K. (1987). *Near-Infrared Technology in the Agricultural and Food Industries*. St. Paul, MN: American Association of Cereal Chemists.
- Williams, C. H., & Steinbergs, A. (1959). Soil sulphur fractions as chemical indices of available sulphur in some Australian soils. *Australian Journal of Agricultural Research*, 10, 340–352.
- Yi, Q. X., Huang, J. F., & Wang, X. Z. (2007). Hyperspectral estimation models for crude fibre concentration of corn. *Journal of Infrared and Millimetre Waves*, 26, 393–395.
- Yoshida, S., Forno, D. A., Cock, D. H., & Gomez, K. A. (1976). *Laboratory manual for physiological studies of rice*. Los Baños, Laguna, Philippines: International Rice Research Institute.
- Zhang, X. J., & Li, M. Z. (2008). Analysis and estimation of the phosphorus content in cucumber leaf in greenhouse by spectroscopy. *Spectroscopy and Spectral Analysis*, 28, 2404–2408.
- Zhang, X., Liu, F., Yong, H., & Gong, X. (2013). Detecting macronutrients content and distribution in oilseed rape leaves based on hyperspectral imaging. *Biosystem Engineering*, 115, 56–65.
- Zhao, D., & Raja Reddy, K. (2003). Corn (*Zea mays* L.) growth, leaf pigment concentration, photosynthesis and leaf hyperspectral reflectance properties as affected by nitrogen supply. *Plant and Soil*, 257, 205–217.
- Zur, Y., Gitelson, A. A., Chvkunova, O. B., & Merzlyak, M. N. (2000). The spectral contribution of carotenoids to light absorption and reflectance in green leaves. In *Proceedings of the second international conference on geospatial information in agriculture and forestry, Lake Buena Vista* (pp. II-17–II-23).